Chemistry of Heterocyclic Compounds, Vol. 41, No. 9, 2005

ELECTROCHEMICAL BEHAVIOR OF INDOLES WITH METHYL, BENZYL, AND DIBENZYL-4-YL GROUPS

I. Buder[1], G. Schwitzgebel[1], Sh. Samsoniya[2], E. Gogritchiani[2], and I. Chikvaidze[2]

2,3-Dimethylindole, N-benzyl-2-methylindole, and 2-(dibenzyl-4-yl)-7-benzylindole (DBBI) under conditions for potentiodynamic electrochemical polymerization (0.3-0.9 V vs. Ag/Ag^+ in acetonitrile) underwent dimerization reactions as was shown by simulation of the potentiodynamic cycles. But DBBI alone polymerized (and only on Au), obviously because of its free N and C(3) positions. This conducting polymer could be technically interesting, because it does not show redox activities in the potential range 0.0-1.1 V vs. the Ag/AgCl electrode.

Keywords: indoles, electropolymerization, cyclic voltammetry, role of substrate in polymeri-zation, simulation of CV.

Indole and some of its derivatives can be polymerized electrochemically. But up to now only a few applications are known, for example, electrodes sensitive to glucose with composite coatings of polyindole and glucose oxidase [1] or to cytochrome C with coatings of 5-carboxyindole [2].

The structure and polymerization mechanism of polyindole (PI) and of its derivatives is controversial [3-7], and even some experimental results seem to be contradictory. It is generally accepted that oxidation generates the indolyl radical cation, which can be deprotonated. MO calculations [6] showed that the unpaired electron and the positive charge are delocalized over the whole indole ring and that structures preserving the aromatic ring should be preferred. The high spin densities at N and C(3) positions seem to present themselves for binding.

Investigations of methylindoles indicate that 3-methylsubstituted indoles do not polymerize [8, 9]. In [10, 11] there was reported polymerization of some methylindoles with free C(3) position, whereas other groups could only detect dimerization and trimerization [8, 9] and assumed that methyl groups in the pyrrole ring were

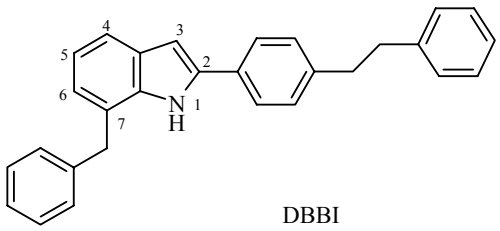

DBBI

[1] FR 8.13. Physical Chemistry, Saarland University, D-66123 Saabrucken, Germany; e-mail: irbu@stud.uni-saarland.de. [2] Department of Organic Chemistry and Chemistry of Natural Compounds. Iv. Javakhishvili Tbilisi State University, 380028 Tbilisi, Georgia; e-mail: shsam@wanex.net. Published in Khimiya Geterotsiklicheskikh Soedinenii, No. 9, pp. 1320-1322, September, 2005. Original article submitted April 4, 2002.

responsible for preventing polymerization. The effect of some other substituents in the pyrrole ring was studied in [6], where the authors did not detect polymerization, and in [12], where the authors polymerized N-methyl-N'-(3-indol-1-ylpropyl)-4,4'-bipyridinium.

This work intends to show that more experimental material is necessary in order to establish the polymerization mechanisms and the specific effects, such as the influence of electrode materials, that are responsible for these mechanisms.

EXPERIMENTAL

The reagents used for the synthesis and the analyses of the other indoles were commercially available products (Aldrich). The products of the synthesis were identified and analytically controlled by ^{1}H NMR, IR, UV and mass spectroscopy. All ^{1}H NMR spectra were collected on a Brüker AM-400 spectrometer (400 MHz) in DMSO-d_6 using TMS as internal standard.

The indole derivatives of this study were 2,3-dimethylindole (DMI), N-benzyl-2-methylindole (N-BMI) and 2-(dibenzyl-4-yl)-7-benzylindole (DBBI). DMI was prepared according to a known method [13].

N-Benzyl-2-methylindole [14]. To a solution of 2-methylindole (1 g, 8.40 mmol) in benzene (80 ml) 50% aqueous KOH (10 ml), benzylchloride (2.50 ml), and tetrabutylammonium bromide (0.15 g) were added. The reaction mixture was stirred at 50-60°C for 4 h. The crude product was purified by column chromatography (silica gel, heptane) to obtain colorless crystals. Yield 0.22 g (13%); mp 47-48°C. UV spectrum (EtOH), λ_{max}, nm (log ε): 208 (4.68), 222 (4.77); 278 (3.95); 292 (3.85). ^{1}H NMR spectrum, δ, ppm: 7.45 (1H, d, J = 7.1, Ar–H); 7.33 (1H, d, J = 7.5, Ar–H); 7.30-7.26 (2H, m, Ar–H); 7.21 (1H, d, J = 7.1, Ar–H); 7.01-6.95 (4H, m, Ar–H); 6.28 (1H, s, H-3); 5.39 (2H, s, CH_2); 2.35 (3H, s, CH_3).

2-(Dibenzyl-4-yl)-7-benzylindole. A mixture of 4-acetyldibenzyl (0.22 g, 1 mmol), N-benzylphenylhydrazine hydrochloride (0.25 g, 1 mmol), and polyphosphoric acid (50 ml) was stirred at 100-110°C for 30-45 min. After cooling, the mixture was poured into cold water (250 ml), extracted four times with Et_2O (25 ml), and dried over Na_2SO_4. The crude product was purified by column chromatography (silica gel, hexane–Et_2O, 50:1) to obtain colorless crystals. Yield 0.07 g (18 %); mp 139-140°C. R_f 0.56 (hexane–ether, 6:1). IR spectrum, cm^{-1}: 3410, 3430 (NH). UV (EtOH), λ_{max}, nm (log ε): 210 (4.61); 249 (4.33); 311 (4.39). ^{1}H NMR spectrum, δ, ppm: 11.09 (1H, s, N–H); 7.83 (2H, d, J = 8.4, Ar–H); 7.36 (1H, d, J = 7.5, H-4); 7.33-7.15 (12H, m, Ar–H); 6.91 (1H, t, J = 7.1, H-5); 6.84 (1H, d, J = 2.24, H-3); 6.80 (1H, d, H-6); 4.32 (2H, s, CH_2–Ph); 2.93 (4H s, CH_2–CH_2). Mass-spectrum, m/z (I, %): M + 387 (25), [M–CHC_6H_5] + 297 (41), [M–$CH_2C_6H_5$] + 206 (2, 1), [M–CHC_6H_5] + 117 (3, 5), [M–CN] + 91 (100). Found, %: C 89.95; H 6.37; N 3.48; M + 387. $C_{29}H_{25}N$. Caclulated, %: C 89.92; H 6.46; N 3.62; M 387.

The Cyclic Voltammetric Measurements were performed in a three-electrode cell at 25.0°C under nitrogen. The reference electrodes were Ag/0.01 M Ag^+ in acetonitrile (Roth HPLC-grade: water content: <0.02%) (0.45 V vs. normal hydrogen electrode (NHE)) for MeCN solutions and Ag/AgCl in 1M NaCl (0.24 V vs. NHE) for aqueous solutions. The electrodes were separated by a diaphragm from the solution. The working electrodes were disks made of Pt (2.0 cm^2), Au (2.0 cm^2), or glassy carbon (GC) (1.3 cm^2). The counter electrode was a Pt disc separated by a diaphragm. The concentration of the indoles was between 0.8 and 2.5 mmol/l. A computer controlled the potentiostat, which modulated the potential and recorded the current. Before and between the measurements, N_2 was bubbled through the solution to remove O_2 and to stir the solution. All polymerization attempts were performed potentiodynamically within specific potential limits (see Results and Discussion).

RESULTS AND DISCUSSION

Potentiodynamic Treatment of DMI. DMI in MeCN solutions was examined at Au, Pt, and GC in the potential field of 0.3-0.7 V with scan rates between 10 and 200 mV/s (Fig. 1). It was irreversibly oxidized, i.e., reduction could not be observed between 10 and 200 mV/s. The peak current of the first oxidation peak (I_{PA}) at E_{PA} = 0.58 V *vs*. the reference electrode (RE) and 50 mV/s is proportional to $\nu^{0.5}$. The peak potential increases

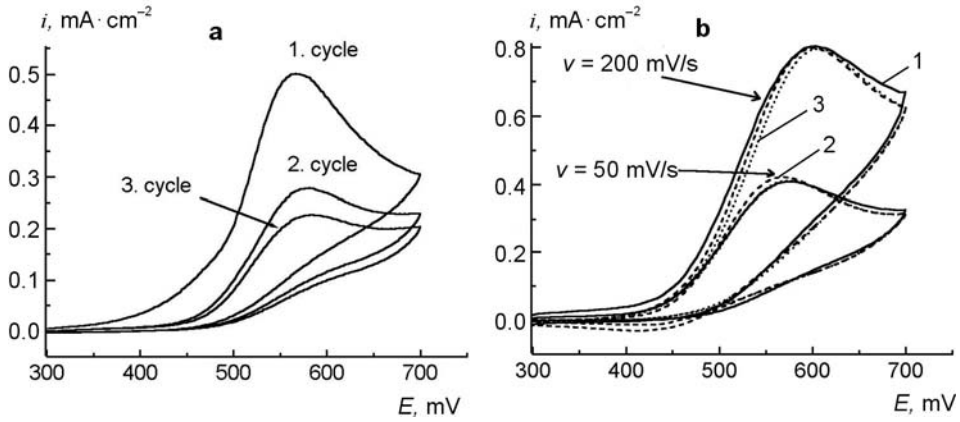

Fig. 1. DMI between 0.3 and 0.7 V.
RE: Ag/Ag^+ (see Experimental); counterelectrode (CE): Pt; *c* (DMI) = 2.5 mmol/l in MeCN; supporting electrolyte: 0.25 M $NaClO_4$. **a** – working electrode (WE): Pt, (A = 2 cm^2); 1.-3. cycles; ν = 50 mV/s; time of measurement was 48 s; the solution was stirred between the cycles; **b** – WE: GC; 1. cycle at different ν; the solution was stirred by bubbling N_2 gas between the measurements for 120 s; time of measurement was 16 s for ν = 50 mV/s and 4 s for ν – 200 mV/s; parameters of simulation (cf. Discussion): $E^1_{1/2}$ = 0.52 V; k^1_{het} = 0.003 cm/s; α^1 = 0.5; $E^2_{1/2}$ = 0.70 V; k^2_{het} = 0.001 cm/s; α^1 = 0.5; k_f = 0.001 mol/l s^{-1}; k_b = 0.0 s^{-1}; D (of all species) = 10^{-5} cm^2/s (1 – measurement, 2 – simulation *a*, 3 – simulation *b*).

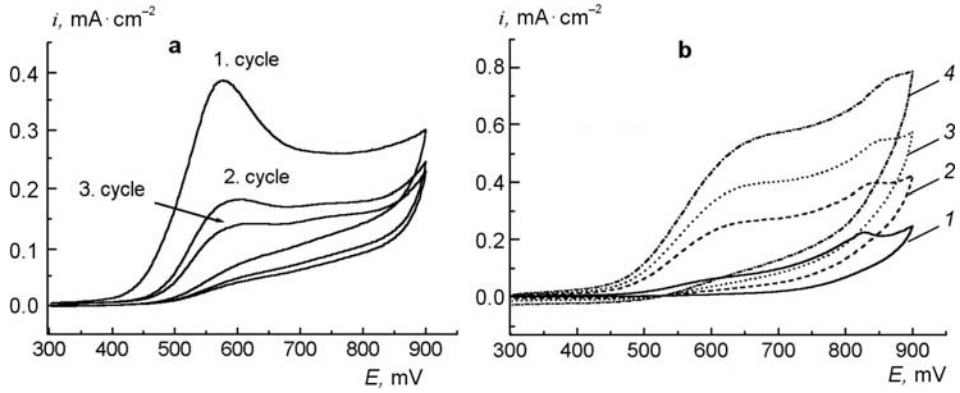

Fig. 2. DMI between 0.3 and 0.9 V.
a – WE: Pt; 1.-3. cycles; ν = 50 mV/s; time of measurement was 72 s; other conditions as in Fig. 1**a**; **b** – WE: GC; 1. cycle at different ν; time of measurement 120 s for 10 mV/s, 24 s for 50 mV/s, 12 s for 100 mV/s, and 6 s for 200 mV/s; other conditions as in Fig. 1**b** (1 – 10, 2 – 50, 3 – 100, 4– 200 mV/s).

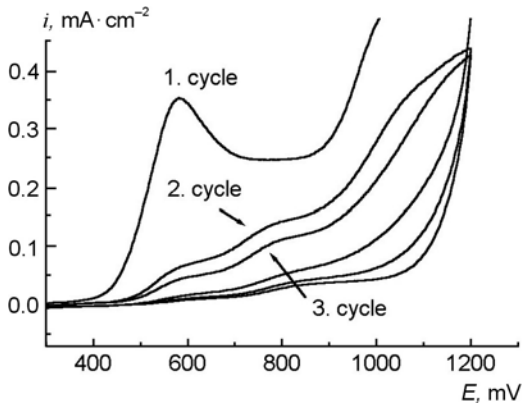

Fig. 3. DMI between 0.2 and 1.2 V.
WE: Pt; 1.-3. cycles; ν = 50 mV/s; time of measurement was 120 s; other conditions as in Fig. 1**a**.

slightly with ν (E_{PA} = 0.56 V for 10 mV/s, E_{PA} = 0.60 V for 200 mV/s), indicating an irreversible electron transfer or trapping of the cation radical by a consecutive chemical reaction. At none of the working electrodes did visible effects occur in this potential range.

In the potential range 0.3-0.9 V a rather flat oxidation peak appeared around 0.8 V at GC (Fig. 2**b**). The study of its *V* dependence was obstructed by the beginning electrode passivation, which at 0.9 V led to an insulating electrode coating (Pt, Au and GC), so that after 10 cycles I drops to zero (Fig. 3).

In the first cycle the current of the coating process is higher than that of the oxidation at lower potentials, indicating a transfer of more than one electron. On the electrode a thin yellowish insulating film was generated, which could be removed in acetone.

Potentiodynamic Treatment of N-BMI. N-BMI was oxidized on gold, platinum and glassy carbon. Compared with DMI the potential of the first oxidation peak is shifted (0.76 V *versus* RE, ν = 50 mV/s) into the positive direction (Fig. 4), but it does not depend on ν (Fig. 4**b**).

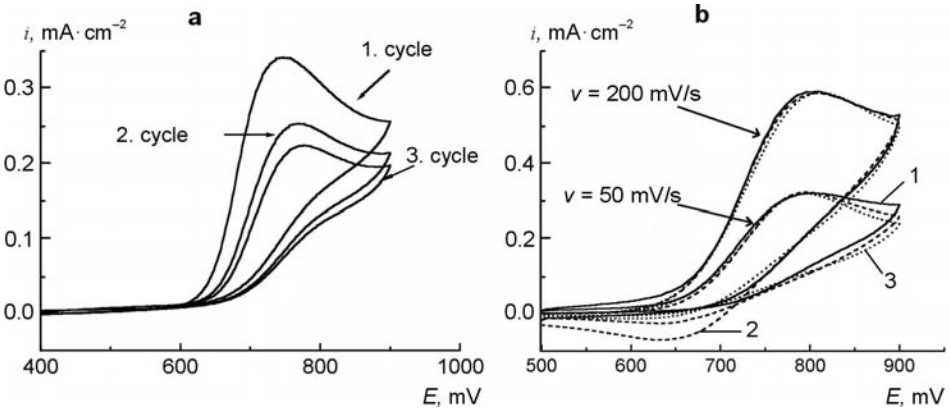

Fig. 4. N-BMI below 0.9 V.
1.5 mmol/l of N-BMI in AN; **a** – WE: Pt; 1.-3. cycles; ν = 50 mV/s; time of measurement was 60 s; other conditions as in Fig. 1**a**; **b** – WE: GC (A = 1.3 cm^2); 1. cycle at different ν; other conditions as in *Fig.* 2**b**; parameters of simulation (cf. Discussion): $E^1_{1/2}$ = 0.72 V; k^1_{het} = 0.0025-0.005 cm/s; α = 0.5; $E^2_{1/2}$ = 0.70 V; k^2_{het} = 0.001 cm/s; α = 0.5; $E^3_{1/2}$ = 0.90 V; k^3_{het} = 0.01cm/s; α = 0.5; k^1_f = 0.01 l/mol·s^{-1}; k^2_f = 0.030 mol/l·s^{-1}; k^1_b = 0.0 s^{-1}; k^2_b = 0.0 s^{-1} (1 – measurement, 2 – simulation *a*, 3 – simulation *b*).

I_{PA} is approximately proportional to $\nu^{0.5}$, and the graph lg I_{PK} vs. lg ν has a slope of 0.46. In this potential range, contrary to DMI, no additional oxidation peaks appeared in the following cycles. The second oxidation peak appeared at 1.1 V (Fig. 5), the current sets in at 0.9 V as for DMI. Similarly to DMI in this potential range, a noticeable passivation was observed due to a thin coating with a golden gleam.

Potentiodynamic Treatment of DBBI. DBBI was irreversibly oxidized on Pt and Au. On Au a brown film was formed (Fig. 6). At the beginning of the coating an oxidation peak at 0.68 V (ν = 50 mV/s) was observed. With increasing cycle number the peak was shifted to higher potentials and finally was superposed by the increasing current at the anodic reversal potential.

Although the cyclovoltammograms of DBBI on Pt were similar as on Au (Fig. 7), only a red coloration but no polymer film appeared. The potential of the oxidation peak is more positive than on Au (0.76 V).

Au electrodes coated with DBBI (positive charge: 0.42 C/cm^2) showed only low electroactivity (Fig. 8**a**), so it is difficult to distinguish it from the cyclovoltammetry (CV) of the blank Au electrode (Fig. 8**b**). Only a small oxidation peak can be assigned to the polymer.

The film on Au is characterized by regular growth at surface defects arranged in stripes, which resulted from cold rolling of the electrode (Fig. 9).

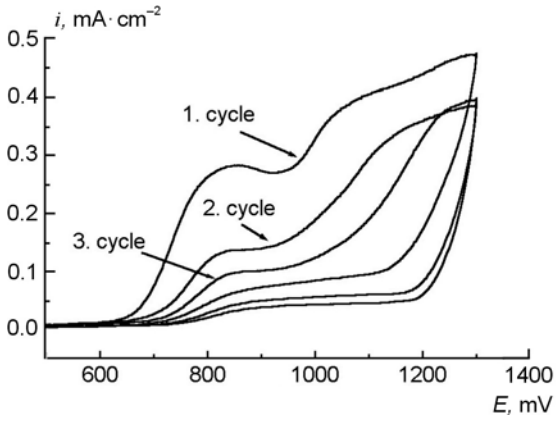

Fig. 5. N-BMI between 0.5 and 1.3 V.
WE: Pt; 1.-3. cycles; time of measurement was 108 s; other conditions as in Fig. 4**a**.

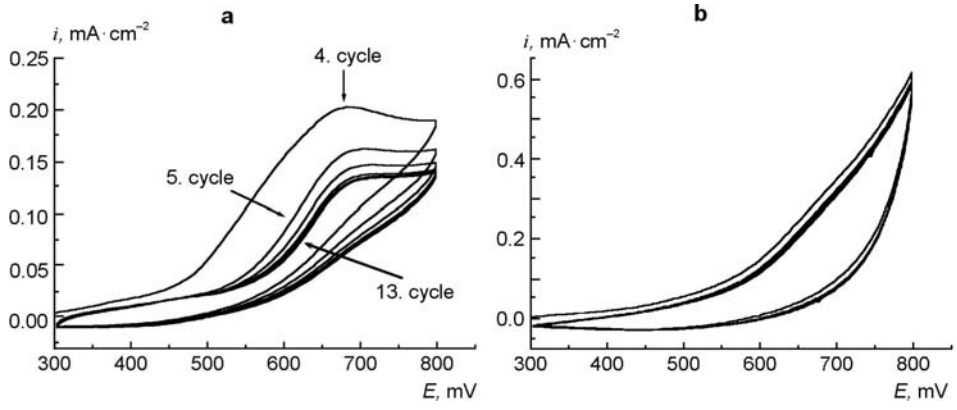

Fig. 6. Polymerization of DBBI on Au.
WE: Au (A = 2 cm^2); 0.8 mmol/l of DBBI in AN; **a** – 4.-13. cycles; time of the measurement was 280 s;
b – 132.-142. cycles; time of the measurement was 47 min 20 s;
the solution was not stirred between the cycles; other conditions as in Fig. 3.

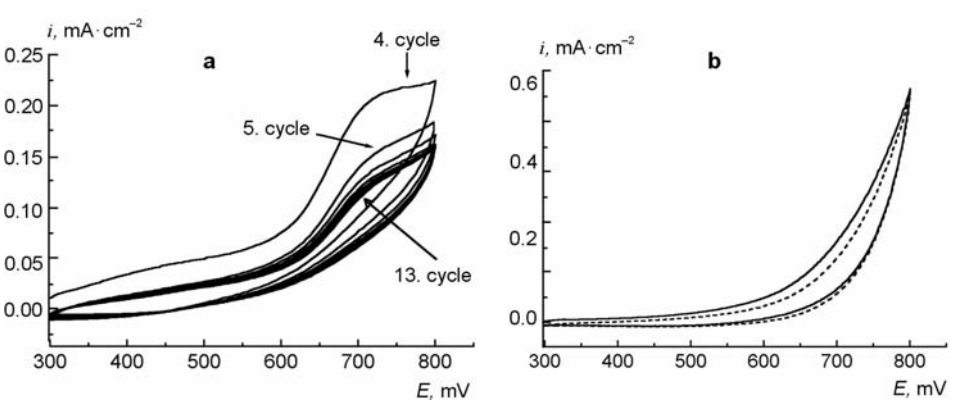

Fig. 7. DBBI on Pt
WE: Pt; **a** – 4.-13. cycles conditions as in Fig. 6**a**; **b** – 125. (solid) and 216. (dash) cycles; conditions as in Fig. 6**b**, but no polymer film was built in spite of continued measurement.

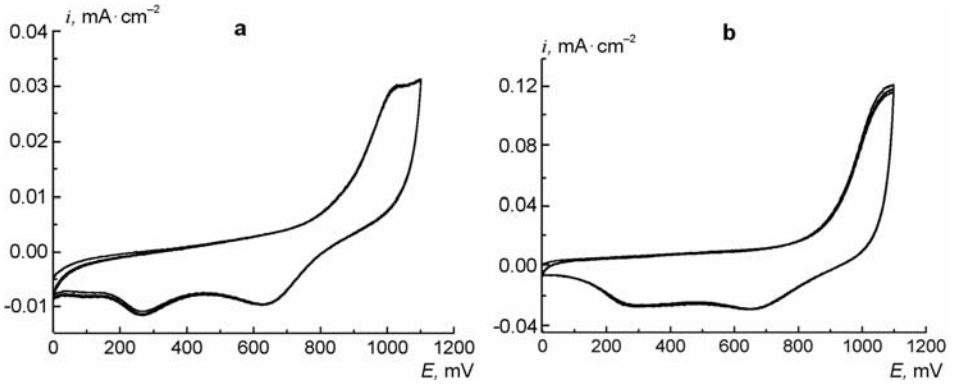

Fig. 8. CV of polymerized DBBI on Au in aqueous solution.
RE: Ag/AgCl in 1M NaCl; CE: Pt; aqueous solution of 0.25 M $NaClO_4$; ν = 50 mV/s; 5 cycles, time of measurement was 220 s, the solution was not stirred between the cycles; **a** – WE: Au coated with polymerised DBBI; **b** – blank Au electrode.

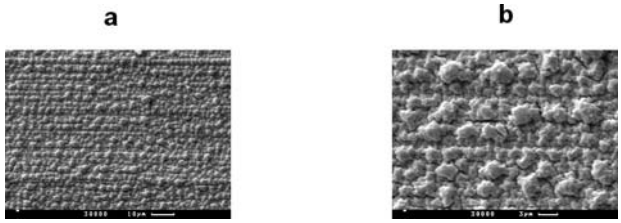

Fig. 9. Raster electron micrograph of DBBI on a rolled Au sheet.
The sample was sputtered with gold; polymerization conditions as in Fig. 6.

General Conclusions. It can be assumed that in a first oxidation step the radical cation of the indoles is formed. The oxidation potential E_{PA} increases from 0.58 V for DMI over 0.68 V at Au and 0.76 V at Pt for DBBI and N-BMI (ν = 50 mV/s). Pronounced reduction could not be observed for any of the indoles, either because of the irreversibility of electron transfer or because of a chemical reaction removing the radical cation.

The lower oxidation potential of DMI is obviously due to the methyl groups in the pyrrole ring, which increase the electrondensity in the rings. In N-BMI the electron-releasing effect of the benzyl group at N is lower. The dibenzyl group at C(2) in DBBI has a similar effect on the electron density of the pyrrole ring.

While DBBI was polymerized on Au, DMI showed no signs of polymerization in this potential range on any electrode. Only at higher potentials was a thin isolating layer formed, which passivated the WE and prevented further electrochemical reactions. In the case of N-BMI the passivation began near the potential of the first oxidation peak.

Both known linking sites of polyindole, N and C(3), are only available for DBBI and only this derivative polymerizes. DMI and N-BMI can dimerize (1,1' and 3,3', respectively), but further polymerization could only occur if the aromatic ring was involved. Therefore, it can be concluded that it is not.

DBBI polymerizes on Au, but not on Pt, probably due to the different adsorption behavior of these materials for monomers, oligomers, and water. The film of DBBI showed almost no electroactivity in aqueous solution, which is unusual for conducting polymers [15, 16]. Apparently the bulky substituents of DBBI inhibit ion exchange by blocking anion as well as cation migration in the polymer matrix. But the film is electrochemically conducting and the oxidative synthesis is not influenced by the film growing (Fig. 6). These properties could qualify poly-DBBI as an interesting electrode material.

SIMULATIONS

The simulations, which are based on widely accepted reaction steps [8-10, 17], were undertaken in order to assign the peaks for mechanistic studies. They were performed with ESP 2.4 developed by C. Nervi and controlled by soft-ware CVSIM in [18]. As a criterion of consistency, we tried to use the same kinetic constants at different scan rates and in different potential ranges for electron transfer (*E*) as well as for homogeneous chemical reaction steps (C).

Simulations of DMI oxidation in the potential range 0.3-0.7 V (Fig. 10) indicated an ECE mechanism, the second electron transfer beginning near the anodic reversal potential of Fig. 1**b** (see Fig. 2**a**). In the potential range 0.3-0.9 V the beginning passivation makes the electron transfer more difficult, resulting in the decrease of the heterogeneous rate constant for the first electron transfer. Because of the high anodic current in this range, a third electron transfer was assumed for the simulation. Only a small cathodic current in the cyclovoltammograms occurred, indicating a second chemical reaction, which traps the oxidation products. The generated dimeric radical cations could react among themselves, with water, or with its oxidation products.

An extended ECE mechanism with dimer concentrations between 0.4 and 0.6 mmol/l in the diffusion layer does not lead to a really good agreement with the experimental curve.

N-BMI forms dimers *via* C(3), which have a similar oxidation potential as monomer, so that no further oxidation peak was observed in the potential range 0.5-0.9 V. The third oxidation process ($E^3_{1/2}$ = 0.9 V vs. RE) can be attributed to the formation of a dication of the dimer as in the case of DMI. With the parameters of Fig. 4**b** a good agreement was achieved.

The proposed reaction mechanism for DBBI (Fig. 11) includes dimerization after forming cation radicals, oxidation of the dimers, chemical reactions between dimer radicals and further oxidation of the tetramers, and so on. Stepwise addition of monomer radicals to dimers did not lead to a successful simulation [19]. The concentration of dimers strongly increases; for example, the concentration in the fourth cycle reaches already 0.3 mmol/l in the diffusion layer.

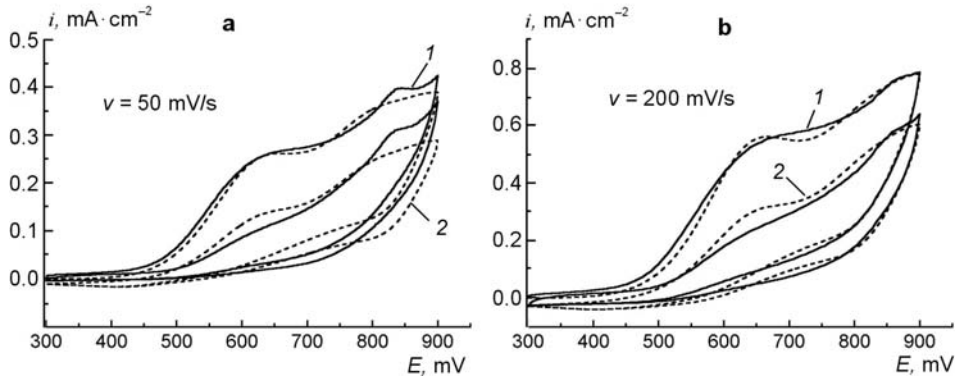

Fig. 10. Simulation of the oxidation of DMI between 0.3 and 0.9 V.
c (DMI): 1.55 mmol/l; *c* (dimer) = 0.4-0.6 mmol/l; k^1_{het} = 0.001 cm^2/s; $E^3_{1/2}$ = 0.85 V;
k^3_{het} = 0.005 cm/s; α^3 = 0.5; k^2_f = 0.005 l/mol·s^{-1}; k^2_b = 0.0 s^{-1};
a – first two cycles at ν = 50 mV/s; time of measurement: 24 s; **b** – first two cycles at ν = 200 mV/s;
time of measurement: 6 s; other parameters of simulation see Fig. 2**b** (1 – measurement, 2– simulation).

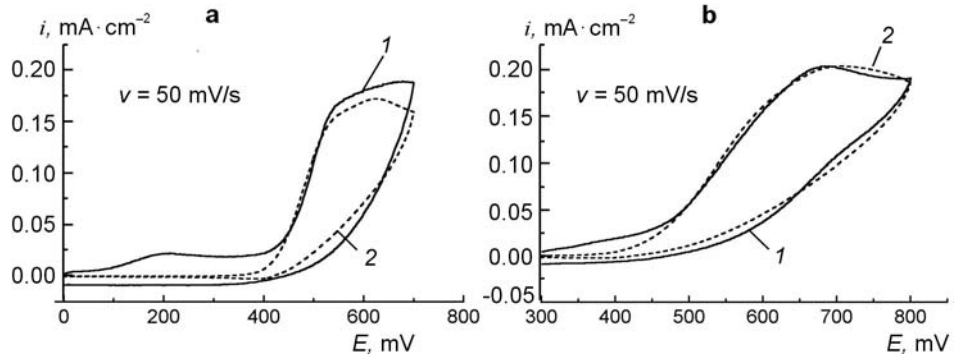

Fig. 11. Simulation of the polymerization of DBBI.
WE: Au; c(DBBI): 0.8 mmol/l; parameters of simulation: $E^1_{1/2}$ = 0.5 V; $E^2_{1/2}$ = 0.6 V;
$E^3_{1/2}$ = 0.7 V; $k^1_{het} = k^2_{het} = k^3_{het}$ = 0.003 cm/s; $\alpha^1 = \alpha^1 = \alpha^3$ = 0.5; $k^1_f = k^2_f = k^3_f$ = 0.1 l/mol·s^{-1};
in the fourth cycle: **a** – 1st cycle, ν = 50 mV/s; **b** – 4th cycle, ν = 50 mV/s;
c (dimer) 0.3 mmol/l (1 – measurement, 2– simulation)

We gratefully acknowledge the financial support of the Deutsche Forschungsgemeinschaft.

REFERENCES

1. P. C. Pandey, *J. Chem. Soc.*, *Faraday Trans. 1*, **84**, 2259 (1988).
2. P. N. Bartlett and J. Farington, *J. Electroanal. Chem.*, **261**, 471 (1989).
3. G. Zotti, S. Zecchin, G. Schiavon, R. Seraglia, A. Berlin, and A. Canavesi, *Chem. Mater.*, **6**, 1742 (1994).
4. P. Jennings, A. C. Jones, A. R. Mount, and A. D. Thomson, *J. Chem. Soc.*, *Faraday Trans.*, **93**, 3791 (1997).

5. H. Talbi, E. B. Maarouf, B. Humbert, M. Alnot, J. J. Ehrhardt, J. Ghanbaja, and D. Billaud, *J. Phys. Chem. Solids*, **57**, 1145 (1996).
6. R. J. Waltman, A. F. Diaz, and J. Bargon, *J. Phys. Chem*., **88**, 4343 (1984).
7. K. Jackowska and J. Bukowska, *Pol. J. Chem.*, **66**, 1477 (1992).
8. A. R. Mount and A. D. Thomson, *J. Chem. Soc.*, *Faraday Trans*., **94**, 553 (1998).
9. A. Berlin, A. Canavesi, G. Schiavon, S. Zecchin, and G. Zotti, *Tetrahedron*, **52**, 7947 (1996).
10. R. Holze and C. H. Hamann, *Tetrahedron*, **47**, 737 (1991).
11. C. H. Hamann, R. Holze, and F. Koeleli, *Dechema Monographie*, **121**, 297 (1990).
12. A. Kelaidopoulou, G. Kokkinidis, and E. Coutouli-Argyropoulou, *Electrochim. Acta*, **43**, 987 (1998).
13. X. Kissman, D. W. Farnsworth, and B. Witkop, *J. Am. Chem. Soc*., **74**, 3948 (1952).
14. R. Garmer, P. A. Albisser, M. A. Penswick, and M. J. Whitehead, *Chem. Ind.*, No. 3, 110 (1974).
15. E. B. Maarouf, D. Billaud, and E. Hannecart, *Mater. Res. Bull*., **29**, 637 (1994).
16. D. Billaud, E. B. Maarouf, and E. Hannecart, *Adv. Sci. Tech. (New Horizonts for Materials*), **4**, 287 (1995).
17. S. W. Kong, K. M. Choi, and K. H. Kim, *J. Phys. Chem. Solids*, **53**, 657 (1992).
18. D. K. Gosser, Jr., *Cyclic Voltammetry and Analyses of Reaction Mechanisms*, VCH, Weinheim, 1993.
19. I. Buder, *Ph.D. Thesis*, Saarbrücken, 2001.